GazeScope: Gaze Target Selection with a Magnifier in VR Environments

Reo Sato
University of Tsukuba
Tsukuba, Japan
rsato@iplab.cs.tsukuba.ac.jp

Taisei Yamaguchi
University of Tsukuba
Tsukuba, Japan
yamaguchi@iplab.cs.tsukuba.ac.jp

Tadatsugu Shibahara
University of Tsukuba
Tsukuba, Japan
shibahara@iplab.cs.tsukuba.ac.jp

Kirk Honda
University of Tsukuba
Tsukuba, Japan
honda@iplab.cs.tsukuba.ac.jp

Myungguen Choi
University of Tsukuba
Tsukuba, Japan
choi@iplab.cs.tsukuba.ac.jp

Buntarou Shizuki
University of Tsukuba
Tsukuba, Japan
shizuki@cs.tsukuba.ac.jp

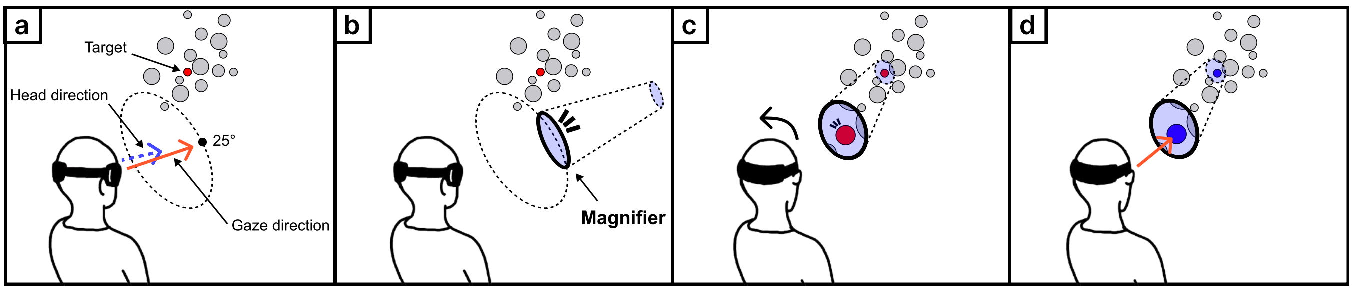

Figure 1: GazeScope is a method that uses a magnifier for selecting small targets in VR environments. The process consists of the following steps: (a) The user gazes at an area 25° away from their head direction. (b) When the user gazes at this area for a certain duration, the magnifier fixed to the user's head activates. (c) The user searches for the target and captures it within the magnifier. (d) The user then selects the target by gazing at it through the magnifier for a certain duration.

Abstract

We present a method for selecting small targets, called GazeScope, which displays a magnifier using gaze and head input. GazeScope allows the user to activate the magnifier by gazing at a point 25° away from the direction of their head. This approach effectively mitigates the Midas touch problem while enabling quick and intentional magnifier activation. The magnifier is fixed to the user's head, allowing the user to direct it toward a target by rotating their head. In this research, we evaluated the improvement in small object selection performance achieved using our method. The results indicate that GazeScope, which displays a fisheye magnifier positioned in front of the user's head, enables accurate selection of small objects that are difficult to select using gaze input alone.

CCS Concepts

• **Human-centered computing** → **Pointing**; **Virtual reality**.

AHs '25, Masdar City, Abu Dhabi, United Arab Emirates

ACM ISBN 979-8-4007-1566-2/25/03
https://doi.org/10.1145/3745900.3746095

Keywords

Virtual reality, Pointing, Eye-gaze interface, Magnification

ACM Reference Format:

Reo Sato, Taisei Yamaguchi, Tadatsugu Shibahara, Kirk Honda, Myungguen Choi, and Buntarou Shizuki. 2025. GazeScope: Gaze Target Selection with a Magnifier in VR Environments. In *The Augmented Humans International Conference 2025 (AHs '25), March 16–20, 2025, Masdar City, Abu Dhabi, United Arab Emirates.* ACM, New York, NY, USA, 14 pages. https://doi.org/10.1145/3745900.3746095

1 Introduction

With the increasing integration of eye trackers into commercial head-mounted displays (HMDs), significant attention has been directed toward gaze interfaces for augmented reality (AR) and virtual reality (VR). By utilizing gaze interfaces, users can interact with distant virtual or real-world objects without using their hands [12, 70]. While gaze modality is superior to other modalities in AR/VR environments in terms of selection speed [46], it still presents several challenges.

A major challenge for gaze interfaces is the selection of small objects. This difficulty arises from gaze estimation errors in eye trackers and involuntary eye movements. The most common approach to addressing this issue is increasing the target size, such as by using magnifiers. In PC environments, many gaze input methods utilizing magnifiers have been proposed, making it easier to select small objects [3, 39, 66–68]. The magnifier serves as a metaphor that allows users to magnify objects intuitively. Additionally, it can magnify objects that cannot be enlarged by the system, such as real-world objects. However, little research has been conducted on implementing magnifiers for selecting small targets using gaze interfaces in AR/VR environments.

One of the challenges in implementing a magnifier as a gaze interface is the difficulty of designing a hands-free gesture to activate the magnifier. In previous methods for mono-modal gaze interfaces with magnifiers, the magnifier appears at the user's current gaze position after dwelling in a specific area for a predetermined duration (dwell time input) [3, 39, 40, 47]. However, using dwell time input as the magnifier activation gesture can lead to unintended activations. This issue, known as the Midas touch problem [30], occurs when the system fails to distinguish between gaze fixation intended for selection and that intended for examination, resulting in accidental input errors. To address this problem, it is generally recommended to use a sufficiently long dwell time, typically between 1000 ms and 2000 ms [50, 79]. While this approach reduces false activations, it significantly increases selection time and negatively impacts usability.

In this research, we present *GazeScope*, a method that allows the user to activate a magnifier using gaze and head, while effectively mitigating the Midas touch problem (Fig. 1). To enable quick magnifier activation while minimizing the Midas touch problem, we utilize the angular region beyond 25° from the user's head direction. When gazing at a position more than 25° away from the head direction, the head generally rotates along with the eyes [62], and the eyes rarely fixate at angles greater than 25° [18, 27]. Hence, since dwelling in this area is an intentional action, the Midas touch problem can be alleviated by using this dwell action as an activation gesture [11, 76]. Furthermore, previous research [11] has shown that this gesture rarely causes the Midas touch problem, even with very short dwell times (200 ms–400 ms). Based on this principle, we designed the activation gesture to involve dwelling gaze within the angular region beyond 25° from the user's head direction for a specified duration. When a user performs the magnifier activation gesture (Fig. 1a), the magnifier is displayed and fixed relative to the user's head (Fig. 1b). The user can then capture targets in the magnifier by rotating their head (Fig. 1c) and selecting the targets using the dwell time input method (Fig. 1d). Thus, GazeScope enables the user to activate the magnifier and select the small target hands-free without causing the Midas touch problem.

In this research, we conducted a user study to examine the appropriate type, arrangement, and size of the magnifier in GazeScope and investigated the selection performance and usability for selecting small objects. The study results revealed that GazeScope, utilizing a large fisheye lens positioned in front of the user's head, is the most suitable configuration. It allows for the accurate selection of small objects with a diameter of 1°, achieving an error rate of 1.19%.

2 Related Work

2.1 Small Object Selection in 3D Environments

2.1.1 Using Hand Modality. Since hands are the most commonly used modality in VR environments, various methods for selecting small objects using hands have been proposed. The most common approach is enlarging the target size [4, 42, 53, 72, 81]. Plasson et al. proposed *RayLens*, a method in which the user controls the magnifier with one hand and selects the target with the other [53]. Additionally, methods have been proposed to extend the *Bubble Cursor* [21]—an approach that implicitly expands the target size using Voronoi tessellation [17]—to 3D environments [4, 42, 72].

When an object is occluded, its reduced visible area makes selection more difficult. As a result, even large objects can be as challenging to select as small ones. One approach to selecting an occluded object is to remove the objects in front of the target [9, 43, 78]. In these methods, a threshold is adjusted using a specific gesture, such as joystick input, to delete objects that are closer to the user than the threshold. Another approach employs the mirror metaphor to provide an alternative perspective on the target, thereby eliminating occlusion [41, 80]. On the other hand, since selecting small occluded objects is particularly challenging, an approach that repositions and resizes objects has been proposed [7, 13, 22, 36, 54, 78]. This approach first selects candidate objects and then rearranges them into easily selectable positions, such as a grid layout [7, 13, 78] or a circular layout [22, 54].

2.1.2 Using Gaze Modality. Most methods for selecting small objects in 3D environments combine gaze modality with other modalities, and few methods rely solely on gaze [33, 52] due to the limited input capabilities of gaze input. As one approach to selecting small objects, methods that correct the cursor position have been proposed [8, 38, 73]. Kyto et al. investigated a method for correcting the gaze cursor position using hands or head movements [38]. Additionally, methods for accurately selecting occluded objects by setting the cursor position to the intersection of the gaze and hand rays have also been proposed [8, 73]. As another approach, two-step selection methods have been proposed, in which candidates are re-positioned and re-sized to a selectable size in the first step [14, 47, 59, 64, 71]. Sidenmark et al. proposed *Cone&Bubble* [64], a method that roughly selects candidates using either the gaze or head ray and then selects a target from the candidates with the other ray.

Most of these methods utilize either the hands or the head as the modality, with head-based methods being superior to hand-based methods, as they are hands-free. Hands-free methods are particularly beneficial for individuals who have difficulty using their hands accurately and can also be useful when a user's hands are occupied. Additionally, the combination of gaze and head modalities enables complex interactions that are difficult to achieve with gaze alone [61, 63]. Overall, multimodal interfaces that combine gaze and head modalities are considered a practical approach for 3D environments.

2.2 Magnifiers in Gaze Interfaces

Magnifiers were initially developed for PC environments as essential assistive tools to help the user, including those with visual impairments, recognize small text and icons on the screen [19, 35, 69]. Standard features in operating systems like Windows and macOS, magnifiers dynamically enlarge specific areas of the screen based on cursor movements, enhancing the information visibility. Over time, magnifiers have evolved into various interface designs that enlarge small details and facilitate the selection of small objects.

In gaze interfaces, methods that use a magnifier to improve visibility by enlarging the scene [1, 40, 45, 74] or selecting small targets [3, 10, 39, 47, 66–68] have been implemented. In most research involving magnifiers in gaze interfaces, the magnifier appears at the user's current gaze position when an activation gesture is performed. Activation gestures are generally classified into two categories. The first category involves using modalities other than gaze, such as keyboards [37], switches [5], touch input [51], or foot input [34], to activate the magnifier. The second category relies on the gaze itself as the activation gesture, with many researches adopting a dwelling action for a specific duration as the activation method [3, 39, 40, 47]. Lankford proposed a two-step dwell-based selection method that activates a zoom window in the first step [39]. Similarly, Ashmore et al. introduced using a fisheye lens as a magnifier [3].

Most research on implementing a magnifier in gaze interfaces within AR/VR environments focuses on improving visibility [1, 40, 45], with little research addressing methods for selecting small targets [47]. For instance, Mutasim et al. investigated the selection performance of a method that displays a magnified view of targets being gazed at, enlarged by a factor of four when a button is pressed or the gaze is fixed for 300 ms [47]. This method can accurately select significantly small targets with diameters of less than 1°. Although this method does not use a magnifier but instead relies on a magnified view of the target, they suggest that using a magnifier can also effectively select small targets in AR/VR environments.

2.3 Adjusting Gaze and Head Direction

In multimodal object selection methods that utilize both gaze and head input, approaches have been proposed in which the head remains fixed in a specific direction, while the gaze moves [38, 44, 59, 61, 64, 67], and vice versa [38, 63, 64]. *Eye&Head* selects a target when the direction of gaze and the head are aligned, effectively mitigating the Midas touch problem [61]. *Radi-Eye* allows users to control a slider with head movements while keeping their eyes fixed on a menu item [63].

As approaches similar to our method, methods that fix a lens to the head and allow users to select objects by looking through the lens have been proposed. Head-based *EyeSeeThrough* is a method for simultaneously selecting menu items and targets by aligning the target with a cockpit menu item fixed to the user's head and selecting it with gaze [44]. The menu items were positioned 20° away from the head direction, and using this method, selections were completed faster than methods where menu items and targets were selected separately. Stellmach et al. proposed *HdLens*, which allows users to select small objects by continuously displaying a magnifier in the direction of the head [67]. This method enables users to easily select small objects in images projected at a distance by utilizing both hand and gaze modalities.

HdLens is similar to our method in that it displays a magnifier fixed to the head and allows small object selection with gaze. However, our method differs from HdLens in that it focuses on selecting small objects in a VR environment, activates the magnifier from a non-activated state, and enables target selection using only gaze without relying on hand input. Furthermore, we contribute by investigating the type, placement, and size of appropriate magnifiers in the subsequent user study.

3 GazeScope

In this research, we present GazeScope, a method that facilitates the selection of small targets in VR environments by displaying a magnifier. This method enables the user to activate the magnifier by dwelling in a specific area 25° away from the user's head direction, where the eyes naturally do not move [18, 27]. This approach can mitigate the Midas touch problem [11, 76] and allows the magnifier to be activated using head and gaze input, making it accessible to individuals who have difficulty moving their hands freely or whose hands are occupied with other tasks. The magnifier is fixed to the user's head, allowing the user to adjust its position by rotating their head. Gaze input is not suitable for continuous adjustments, such as positioning a magnifier, due to its lack of accuracy. To enable precise magnifier positioning, we utilize head input, which is more suitable for continuous control [63].

GazeScope involves two main steps:

(1) **Magnifier Activation**: The user dwells in a specific area 25° away from their head direction for a certain period. Afterward, a magnifier anchored to the user's head is displayed.
(2) **Target Selection**: The user rotates their head to capture the target into the magnifier. The target is selected by gazing at it within the magnifier for a certain period.

3.1 Magnifier

In this research, we designed GazeScope using linear and fisheye lenses as magnifiers.

3.1.1 Linear Lens. A linear lens magnifies objects concentrically by a factor of n. The lens is commonly used in various studies and applications [1, 37, 39, 40, 74]. While linear lenses provide uniformly magnified images, they obscure part of the background [32]. Consequently, when using a linear lens as a magnifier in our method, there is a risk that the magnifier may block the target.

3.1.2 Fisheye Lens. A fisheye lens displays the entire image within the lens by distorting the magnified area [20]. This allows the peripheral regions of the magnifier to blend with the background, preventing the magnifier from obstructing targets in our method. As a result, the target remains within the user's field of view (FOV), enabling them to capture it in the magnifier immediately. The appearance of fisheye lens images varies depending on the projection equations, which typically transform the original images into smoothly distorted representations, such as stereographic or orthographic projections [32]. However, fisheye lenses based on these projections generally exhibit a small area of significant magnification, making them unsuitable for target selection [3, 23]. To address this limitation, a hybrid lens combining linear magnification at the lens's center and non-linear magnification at the edges was implemented [2, 56, 57]. This lens provides a large linear magnification area by intentionally distorting the edges of the lens (Fig. 2a). In this research, we employed the following projection equation for the fisheye lens (Fig. 2b):

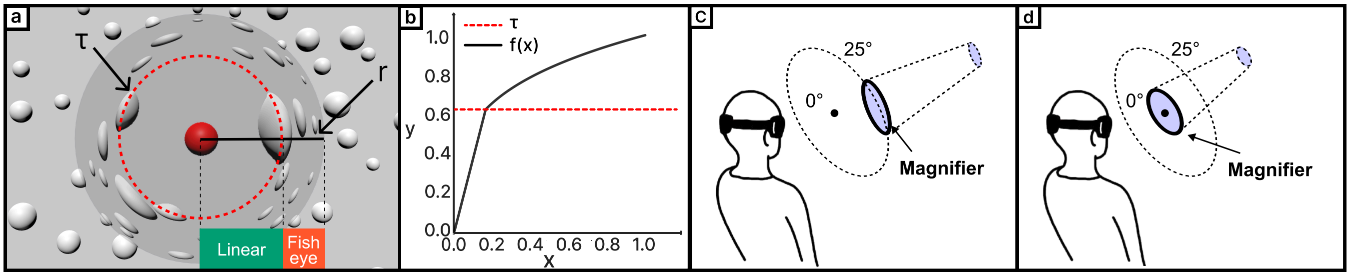

Figure 2: GazeScope designs for fisheye lens and lens positions. (a) Image of a fisheye lens. (b) Schematic illustration of the projection equation. (c) The lens is positioned at the location where the magnifier activation gesture is performed (25° away from the user's head direction). (d) The lens is positioned directly in front of the user's head, aligned with the head direction.

$$f(x) = \begin{cases} nx, & \text{if } x \leq \tau, \\ x^{1/n}, & \text{if } \tau < x \leq r \end{cases} \quad \text{where,} \quad \tau = r \times n^{\frac{1}{1-n}} \tag{1}$$

Here, r represents the lens's radius, x denotes the distance from the center, and n is the magnification factor. τ is the threshold between linear magnification and fisheye magnification. By using τ, the two functions in Equation 1 are smoothly connected at τ. However, the area expanded by a factor of n remains smaller with the fisheye lens compared to the linear lens.

3.2 Lens Position

Magnifiers in gaze interfaces are typically positioned at the user's gaze point when performing activation gestures. In our method, it is also natural for the magnifier to appear in the area where the activation gesture is performed (Fig. 2c). However, a 25° angle from the front of the head may impair ocular kinematics [65], potentially making it difficult to select targets within the magnifier.

To address this issue, we adopt an approach that activates the magnifier directly in front of the user's head [67] (Fig. 2d). This approach shifts the interaction space to the front of the user's head, enabling more comfortable gaze fixation. However, the discrepancy between the gaze position after magnifier activation and the magnifier's display position may negatively affect target selection performance. To examine this, we conducted a comparative study to identify the optimal position for displaying the magnifier.

4 Study

We conducted a user study to investigate 1) whether our method facilitates the selection of small targets in a VR environment and 2) the appropriate design parameters for the magnifier in our method.

4.1 Apparatus and Participants

We used the HTC Vive XR Elite HMD with the HTC VIVE full-face tracker. According to its specifications, the eye tracker has an accuracy between 0.5° and 1.1°, a visible FOV of 110°, and the HMD and the eye tracker's refresh rate of 90 Hz. The application used in the study was developed in Unity Version 2023.2.11f1.

Twenty-four participants (four females, 20 males; mean age = 22.8 years, SD = 0.9 years; ID: P1–P24) from a local university were enrolled. All participants had normal color vision. Among them, 12 had normal vision, six wore glasses, and six wore corrective lenses. Participants wearing glasses removed them and adjusted the diopter dial on the HMD. Five participants had prior experience with an eye-tracking interface. Every participant received 16 USD, and each study took approximately 60 minutes.

4.2 Implementation

In this study, the magnifier activation gesture is defined as dwelling in a circular area positioned at 25° eccentricity and 30° azimuth (Fig. 3b) from the participants' head direction for 400 ms. The radius of the area was set to 5°. For consistency across all conditions, this activation gesture was used throughout. Since users fixate on this position only approximately 0.3% of the time [76], the likelihood of accidentally performing an activation gesture while searching for a target is low. Given that the range of eye movement is wider at the bottom and narrower at the top [77], we selected this position for the activation gesture, as it is close to the center of the face and less likely to trigger the Midas touch. Since multiple candidate positions exist, our selected position is not necessarily the optimal choice. However, because this study focuses on selection performance using a magnifier rather than optimizing the activation gesture position, we adopted this location.

In the initial implementation, we did not provide feedback to indicate the dwelling position for the activation gesture. However, since accurately dwelling at the intended position without feedback is challenging, we introduced a marker at that position. The marker was a black circle with a 0.5° radius, positioned at 1.0 m from the participant's head. When the magnifier was activated, the marker disappeared.

The lens's magnification factor was set to four. Thus, in the fisheye lens, the area within 0.63 times the lens's radius from the center functioned as a linear lens with a fourfold magnification factor. The magnifiers were displayed at 1.0 m from the participant's head. A target was selected by dwelling on the object within the magnifier for 600 ms. In other words, objects outside the magnifier could not be selected. Ideally, it would be preferable to select a target without activating the magnifier and to activate it only when selecting small objects. However, because our goal was to investigate the selection performance of our method when using the magnifier, we implemented the system in this way.

4.3 Design

We used a within-participant design. There are four independent variables (Fig. 3):

- *Lens Type*: Linear, Fisheye
- *Lens Position*: Center, Upper-Right
- *Lens Width*: 24°, 32°, 40°
- *Target Width*: 1°, 2°, 3°

Lens Type refers to the type of magnifier used (Fig. 3a). *Lens Position* refers to the location where the magnifier appears (Fig. 3b). The Center position corresponds to the front of the user's head, while the Upper-Right position corresponds to the location of the dwelling position used to activate the magnifier (25° eccentricity and 30° azimuth). *Lens Width* refers to the diameter of the magnifier (Fig. 3c). In the linear lens, a larger lens width increases the magnification area but also enlarges the area hidden by the lens. The larger hidden area may make it more challenging to capture the target within the lens. Thus, we adopted this value to investigate the trade-off between the magnification and the hidden area's size. Since the range of motion of the human eye is approximately 45°, the maximum radius of the lens from which the peripheral area remains visible is about 20° when the lens is positioned at the Upper-Right position. Therefore, we set the upper limit at 40° and selected values of 24° and 32°, which are below this threshold. *Target Width* refers to the diameter of the target. Orquin et al. [49] found that, even with a high-accuracy eye tracker, a target size of 5° or more is necessary to capture a high proportion of gaze fixations on the target. Similarly, Feit et al. [16] reported that a target size of 2.91° × 3.33° is sufficient for 75% of users in gaze interfaces. Therefore, a *Target Width* of 1° and 2° is considered small, while 3° is classified as medium.

The order of the *Lens Type* × *Lens Position* was counterbalanced using a Latin square. The order of *Lens Width* was also counterbalanced. Each participant experienced the tasks in the same order of *Lens Width* for all *Lens Type* × *Lens Position*. Participants experienced 21 trials (3 *Target Width* × 7) for each *Lens Type* × *Lens Position* × *Lens Width*. The order of the 21 trials was random. Finally, we collected 2 *Lens Type* × 2 *Lens Position* × 3 *Lens Width* × 21 trials = 252 valid object selection datasets for each participant (6,048 datasets in total with 24 participants).

4.4 Procedure and Task

First, we greeted the participants and briefly introduced them to the study. All participants provided written and informed consent. We then offered detailed task instructions through graphical images. When the participants wore an HMD, they performed a five-point eye-tracking calibration of the software initially installed on the HMD. Before the main sessions started, all participants engaged in a practice session using different parameters.

The task involved selecting a target using magnifiers in a VR environment. During the task, 100 selectable objects were displayed. The target was a red sphere, while the other objects were white spheres. The width of the target was set to the *Target Width* value, whereas the widths of the other objects were randomly assigned values between 1.0° and 3.0°. Each object was placed at a random location between 2.0 m and 4.0 m from the participant, ensuring no objects were visually overlapped. A gaze cursor, a green circle with a diameter of 0.2°, was displayed during the task. We applied a saccade detection [16] with a triangular kernel filter [31] to the gaze data.

Participants were required to select targets quickly and accurately using GazeScope. When the objects in the magnifier were gazed at, the color of the gazed object changed to blue. A selection error was defined as a trial in which participants either selected a non-target object or failed to select within 10 s of the trial's initiation. As feedback, a sound corresponding to a correct or incorrect selection was played when the target was selected. The objects were regenerated when a selection occurred or when the target was not selected within 10 s of the trial's initiation. The objects were regenerated at random locations 20° from the previous target generation location and within a 30° radius centered on the frontal direction of the torso. Each trial consisted of this task, and the same procedure was repeated for subsequent trials.

Participants experienced three *Lens Width*s in succession for a specific *Lens Type* × *Lens Position*. All trials of one combination of *Lens Type* and *Lens Position* were completed, and they were asked to fill out the System Usability Scale (SUS) [6] and NASA Task Load Index (NASA-TLX) [24]. This procedure was repeated four times, associated with the combination of *Lens Type* and *Lens Position*. After completing all trials, participants were interviewed and asked to indicate their *Lens Type* × *Lens Position* of preference.

4.5 Metrics

An analysis was conducted on the following metrics:

Error Rate: This denotes the failure rate of all trials, where a trial was considered erroneous if the selection was the non-target object or if no selection was made within 10 s of the trial's initiation.

Target Search Time: The time elapsed from the magnifier's activation to the target's first appearance within the magnifier (Fig. 4a). If the target is already displayed in the magnifier when activated, this value will be zero.

Target Selection Time: The time elapsed from the target's appearance in the magnifier to the successful selection of the target (Fig. 4b).

Total Selection Time: The total time elapsed from the initiation of a trial to the successful target selection (Fig. 4c).

Usability Questionnaire: This provides subjective feedback, through SUS and NASA-TLX questionnaires, to measure usability and workload in terms of user strain for each *Lens Type* × *Lens Position*. Furthermore, all participants completed a questionnaire to indicate their preferences for *Lens Type* × *Lens Position*.

5 Result

The error rate, target search time, target selection time, and total selection time did not follow a normal distribution. A nonparametric aligned rank transformation (ART) method [25, 55, 75] was applied to these datasets, followed by a four-way repeated measures ANOVA with *Lens Type*, *Lens Position*, *Lens Width*, and *Target Width* as factors. For the SUS and NASA-TLX scores, we applied the ART, as Likert scales are considered ordinal. A two-way repeated measures ANOVA was then conducted with *Lens Type* and *Lens Position* as factors. Within-factor post-hoc analyses were conducted using ART-C [15] with Holm correction [26]. The results of the statistic

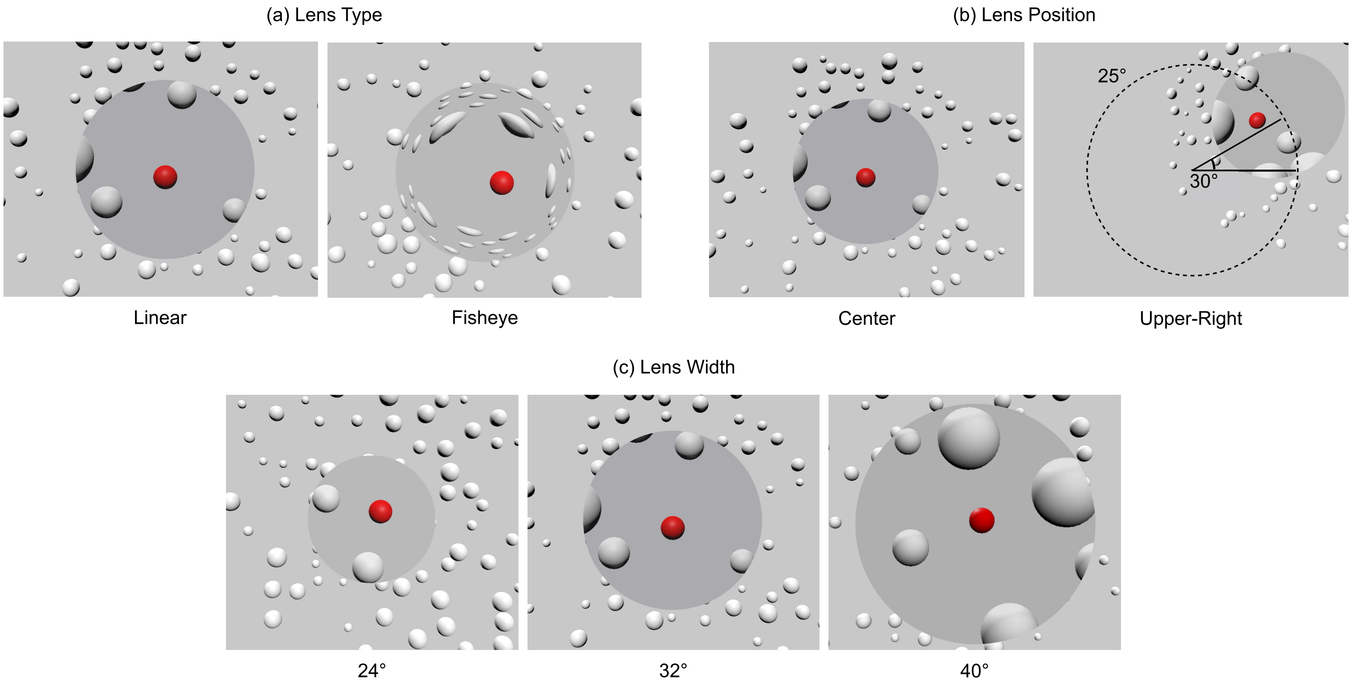

Figure 3: Independent variables. The red object represents the target, with a width of 1°.

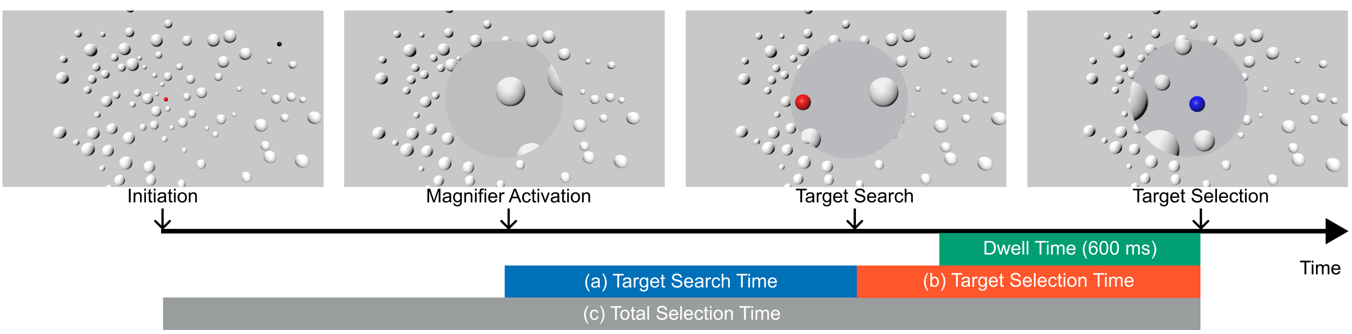

Figure 4: The definition of (a) target search time, (b) target selection time, and (c) total selection time.

analysis are shown in Table 1. We have defined abbreviations for each *Lens Type* × *Lens Position* condition as follows: Linear × Center is denoted as LC, Linear × Upper-Right as LU, Fisheye × Center as FC, and Fisheye × Upper-Right as FU.

5.1 Error Rate

The error rates of each *Lens Type* × *Lens Position* (LC, LU, FC, FU) were 2.31%, 4.70%, 1.12%, and 5.82%, respectively (lower is better). Among these, the timeout error rates were 1.65%, 3.31%, 0.93%, and 5.09%, respectively. Therefore, timeout errors were the most common cause of the errors. The number of trials resulting in timeout errors without magnifier activation accounted for 0.15% of the total (9 out of 6,048 trials).

For *Lens Width*, the lowest error rate was observed when selecting targets with a *Target Width* of 1°: for LC, when the *Lens Width* was 24° (1.79%); for LU and FU, when the *Lens Width* was 32° (6.55% and 10.12%, respectively); and for FC, when the *Lens Width* was 40° (1.19%).

The statistical analysis results are shown in Table 1a. Significant main effects were found for *Lens Type* ($p < .01$), *Lens Position* ($p < .01$), *Lens Width* ($p < .01$), and *Target Width* ($p < .01$). These results indicate that the Center condition had a significantly lower error rate than the Upper-Right condition. Within-factor post-hoc analyses revealed that larger *Lens Width* values resulted in lower error rates for the LU, FC, and FU. However, for LC, the smallest *Lens Width* condition (24°) had a significantly lower error rate. The error rates are shown in Fig. 5.

Table 1: The results of the ANOVA for (a) Error Rate, (b) Target Search Time, (c) Target Selection Time, (d) Total Selection Time, (e) System Usability Scale (SUS), and (f) NASA Task Load Index (NASA-TLX). Due to space limits, *Lens Type*, *Lens Position*, *Lens Width*, and *Target Width* are indicated as LT, LP, LW, and TW, respectively.

(a) Error Rate

Factor	F value	p	η_p^2
LT	$F_{1,5989} = 1220.95$	**<.01**	.169
LP	$F_{1,5989} = 2307.52$	**<.01**	.278
LW	$F_{2,5989} = 1129.38$	**<.01**	.274
TW	$F_{2,5989} = 615.85$	**<.01**	.171
LT × LP	$F_{1,5989} = 410.92$	**<.01**	.064
LT × LW	$F_{2,5989} = 98.48$	**<.01**	.032
LP × LW	$F_{2,5989} = 663.38$	**<.01**	.181
LT × TW	$F_{2,5989} = 251.65$	**<.01**	.078
LP × TW	$F_{2,5989} = 811.79$	**<.01**	.213
LW × TW	$F_{4,5989} = 766.63$	**<.01**	.339
LT × LP × LW	$F_{2,5989} = 50.37$	**<.01**	.017
LT × LP × TW	$F_{2,5989} = 729.60$	**<.01**	.196
LT × LW × TW	$F_{4,5989} = 187.47$	**<.01**	.111
LP × LW × TW	$F_{4,5989} = 696.26$	**<.01**	.317
LT × LP × LW × TW	$F_{4,5989} = 166.70$	**<.01**	.100

(b) Target Search Time

Factor	F value	p	η_p^2
LT	$F_{1,5778} = 296.10$	**<.01**	.049
LP	$F_{1,5778} = 2.98$	.08	.001
LW	$F_{2,5778} = 5.10$	**<.01**	.002
TW	$F_{2,5778} = 194.68$	**<.01**	.063
LT × LP	$F_{1,5778} = 0.12$	.73	.000
LT × LW	$F_{2,5778} = 0.87$	.42	.000
LP × LW	$F_{2,5778} = 5.96$	**<.01**	.002
LT × TW	$F_{2,5778} = 1.36$	.26	.000
LP × TW	$F_{2,5778} = 0.54$	.58	.000
LW × TW	$F_{4,5778} = 1.08$	.37	.001
LT × LP × LW	$F_{2,5778} = 0.88$	.42	.000
LT × LP × TW	$F_{2,5778} = 0.13$	.88	.000
LT × LW × TW	$F_{4,5778} = 0.93$	.45	.001
LP × LW × TW	$F_{4,5778} = 0.26$	.91	.000
LT × LP × LW × TW	$F_{4,5778} = 1.91$	.11	.001

(c) Target Selection Time

Factor	F value	p	η_p^2
LT	$F_{1,5779} = 95.00$	**<.01**	.016
LP	$F_{1,5778} = 289.82$	**<.01**	.048
LW	$F_{2,5778} = 36.39$	**<.01**	.012
TW	$F_{2,5779} = 380.87$	**<.01**	.116
LT × LP	$F_{1,5779} = 74.59$	**<.01**	.013
LT × LW	$F_{2,5778} = 13.08$	**<.01**	.005
LP × LW	$F_{2,5778} = 29.74$	**<.01**	.011
LT × TW	$F_{2,5778} = 15.39$	**<.01**	.005
LP × TW	$F_{2,5778} = 45.05$	**<.01**	.015
LW × TW	$F_{4,5778} = 7.21$	**<.01**	.005
LT × LP × LW	$F_{2,5778} = 11.69$	**<.01**	.004
LT × LP × TW	$F_{2,5779} = 8.97$	**<.01**	.003
LT × LW × TW	$F_{4,5778} = 4.58$	**<.01**	.003
LP × LW × TW	$F_{4,5778} = 6.18$	**<.01**	.004
LT × LP × LW × TW	$F_{4,5778} = 3.62$	**<.01**	.002

(d) Total Selection Time

Factor	F value	p	η_p^2
LT	$F_{1,5778} = 36.83$	**<.01**	.006
LP	$F_{1,5778} = 82.59$	**<.01**	.014
LW	$F_{2,5778} = 1.51$	.22	.001
TW	$F_{2,5778} = 467.74$	**<.01**	.139
LT × LP	$F_{1,5778} = 8.56$	**<.01**	.001
LT × LW	$F_{2,5778} = 10.70$	**<.01**	.004
LP × LW	$F_{2,5778} = 0.22$	.80	.000
LT × TW	$F_{2,5778} = 4.57$	**<.05**	.002
LP × TW	$F_{2,5778} = 9.97$	**<.01**	.003
LW × TW	$F_{4,5778} = 1.05$	.38	.001
LT × LP × LW	$F_{2,5778} = 8.85$	**<.01**	.003
LT × LP × TW	$F_{2,5778} = 5.04$	**<.01**	.002
LT × LW × TW	$F_{4,5778} = 1.48$	.21	.001
LP × LW × TW	$F_{4,5778} = 0.62$	.65	.000
LT × LP × LW × TW	$F_{4,5778} = 0.35$	.84	.000

(e) System Usability Scale (SUS)

Factor	F value	p	η_p^2
LT	$F_{1,69} = 1.88$	.17	.027
LP	$F_{1,69} = 53.76$	**<.01**	.438
LT × LP	$F_{1,69} = 0.06$	.81	.001

(f) NASA Task Load Index (NASA-TLX)

Factor	F value	p	η_p^2
LT	$F_{1,69} = 1.79$	.19	.025
LP	$F_{1,69} = 24.81$	**<.01**	.264
LT × LP	$F_{1,69} = 2.07$	.16	.029

5.2 Target Search Time

The target search time of each *Lens Type* × *Lens Position* (LC, LU, FC, FU) was 1.52 s, 1.47 s, 1.11 s, and 1.18 s, respectively (lower is better). The statistical analysis results are shown in Table 1b. Significant main effects were found for *Lens Type* ($p < .01$), *Lens Width* ($p < .01$), and *Target Width* ($p < .01$); however, *Lens Position* ($p = .08$) did not show significant main effects. These results indicate that the Fisheye condition had a significantly faster target search time than the Linear condition. The target search time is shown in Fig. 6.

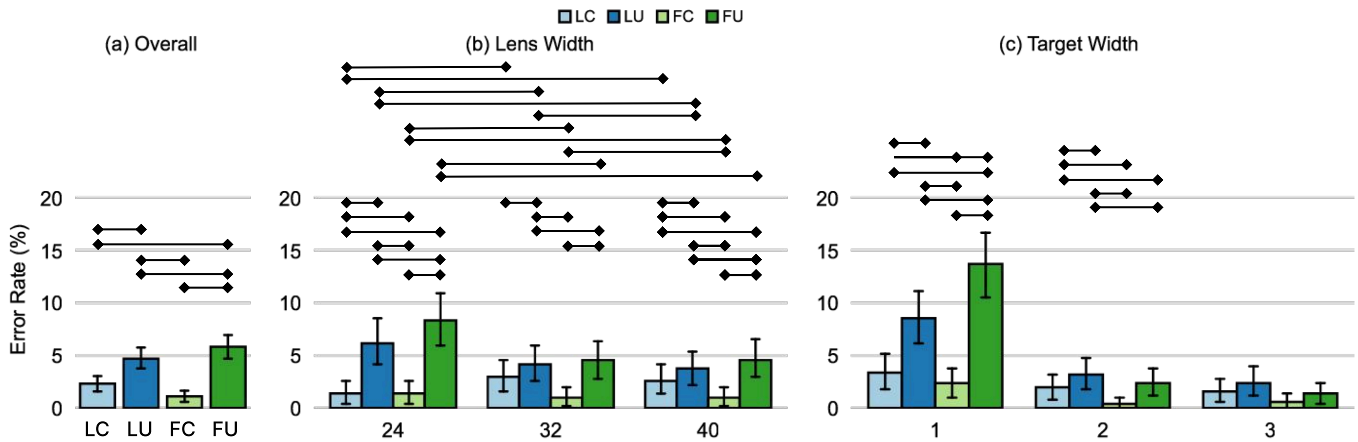

Figure 5: Error rate. The error bars represent the standard error. Statistically significant differences are indicated with solid lines for $p < .05$.

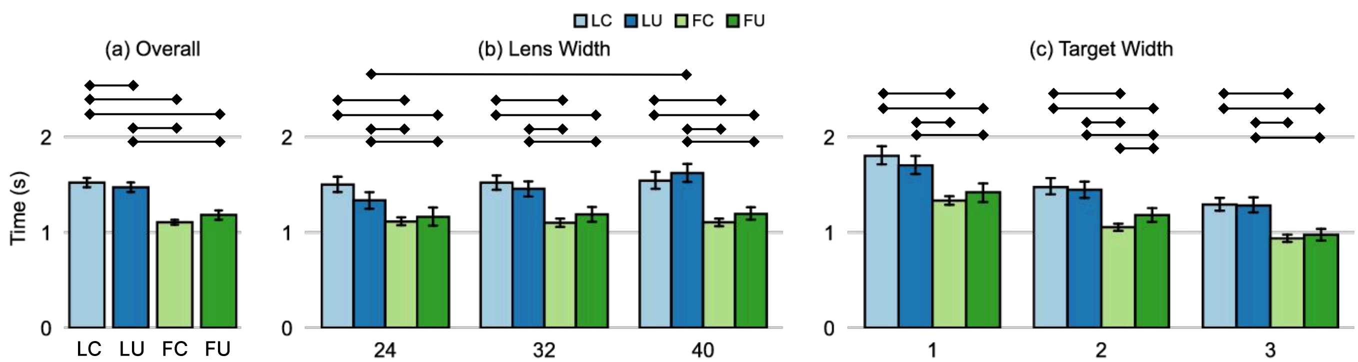

Figure 6: Target search time. The error bars represent the standard error. Statistically significant differences are indicated with solid lines for $p < .05$.

5.3 Target Selection Time

The target selection time of each *Lens Type* × *Lens Position* (LC, LU, FC, FU) was 1.02 s, 1.29 s, 1.12 s, and 1.64 s, respectively (lower is better). The statistical analysis results are shown in Table 1c. Significant main effects were found for *Lens Type* ($p < .01$), *Lens Position* ($p < .01$), *Lens Width* ($p < .01$), and *Target Width* ($p < .01$). These results indicate that the Linear condition resulted in a significantly faster target selection time than the Fisheye condition. Additionally, the Center condition led to a significantly faster target selection time than the Upper-Right condition. The target selection time is shown in Fig. 7.

5.4 Total Selection Time

The total selection time of each *Lens Type* × *Lens Position* (LC, LU, FC, FU) was 4.03 s, 4.21 s, 3.73 s, and 4.19 s, respectively (lower is better). The statistical analysis results are shown in Table 1d. Significant main effects were found for *Lens Type* ($p < .01$), *Lens Position* ($p < .01$), and *Target Width* ($p < .01$); however, *Lens Width* ($p = .22$) did not show significant main effects. These results indicate that the Fisheye condition resulted in a significantly faster total selection time than that of the Linear condition. Additionally, the Center condition led to a significantly faster total selection time than the Upper-Right condition. The total target selection time is shown in Fig. 8.

5.5 System Usability Scale (SUS)

The overall SUS score of each *Lens Type* × *Lens Position* (LC, LU, FC, FU) was 73.54, 56.04, 77.50, and 57.60, respectively (higher is better). The statistical analysis results are shown in Table 1e. We observed that *Lens Position* ($p < .01$) had significant main effects; however, *Lens Type* ($p = .17$) did not show significant main effects. The SUS score of all *Lens Type* × *Lens Position* is shown in Fig. 9a.

5.6 NASA Task Load Index (NASA-TLX)

The overall workload score of each *Lens Type* × *Lens Position* (LC, LU, FC, FU) was 44.44, 53.51, 38.40, and 55.03, respectively (lower is better). The statistical analysis results are shown in Table 1f. We observed that *Lens Position* had significant main effects in all NASA-TLX items; however, *Lens Type* did not show significant main effects. The workload score of all *Lens Type* × *Lens Position* is shown in Fig. 9b.

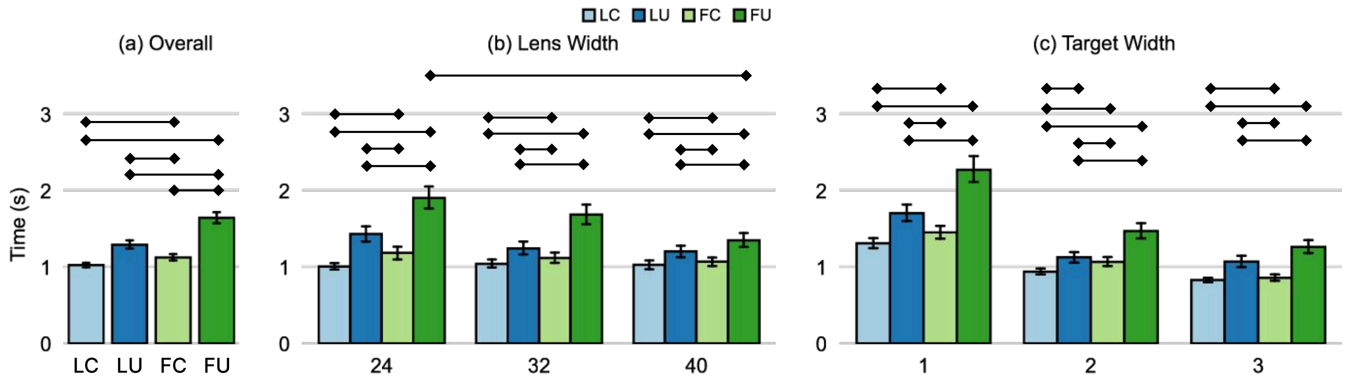

Figure 7: Target selection time. The error bars represent the standard error. Statistically significant differences are indicated with solid lines for $p < .05$.

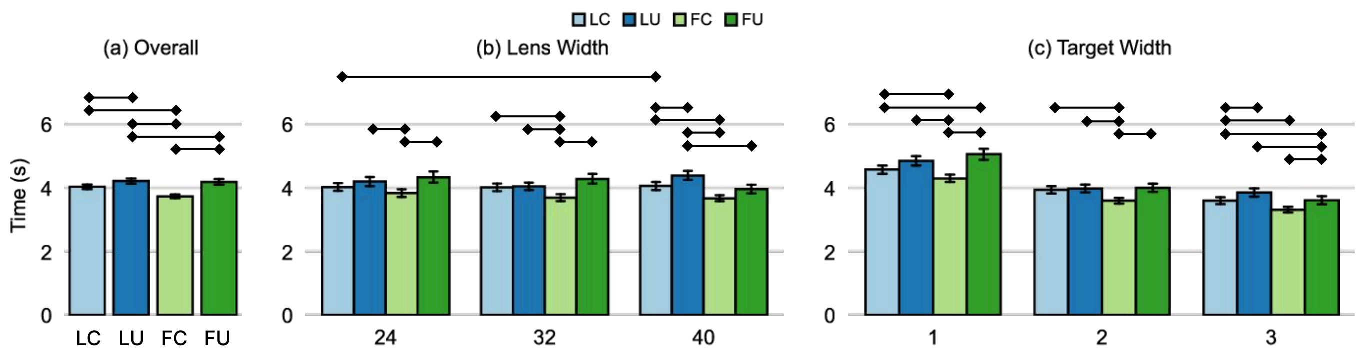

Figure 8: Total selection time. The error bars represent the standard error. Statistically significant differences are indicated with solid lines for $p < .05$.

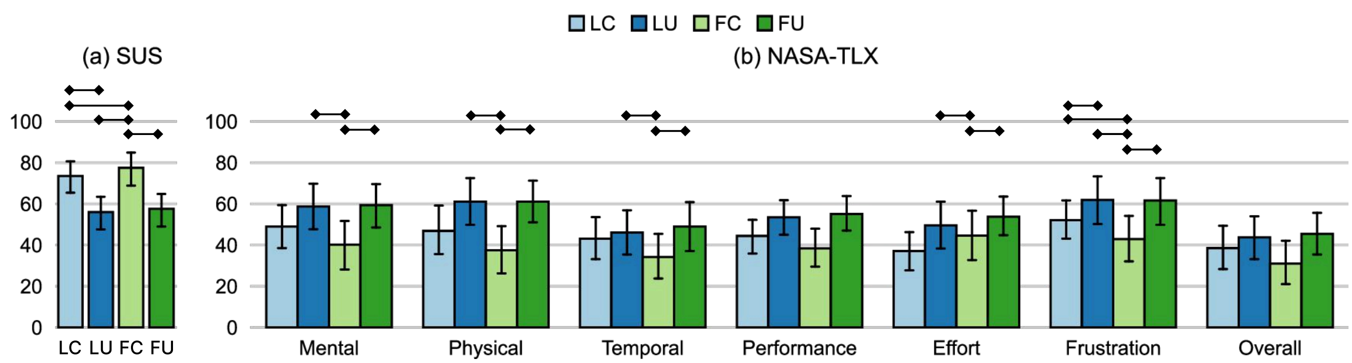

Figure 9: (a) SUS and (b) NASA-TLX. The error bars represent the standard error. Statistically significant differences are indicated with solid lines for $p < .05$.

5.7 Participants' Feedback

5.7.1 Participants' Preference. The average rank of preference for each *Lens Type* × *Lens Position* (LC, LU, FC, FU) was 2.17, 3.33, 1.42, and 3.08, respectively (lower is better). Thus, FC, LC, FU, and LU were preferred in that order.

5.7.2 Lens Type. Some participants preferred the linear lens to the fisheye lens. P7 commented, *"The linear lens was preferred to the fisheye lens because it made target selection easier."* P11 remarked, *"The LC was the easiest to get accustomed to. In contrast, the fisheye lens was much more difficult to operate than I had anticipated."* However, some participants (P12, P18, P20, P22) criticized the linear lens for completely hiding the target. P18 commented, *"If the target is* *hidden behind the magnifier and not visible, it becomes difficult to search the target."*

Many participants left positive comments about the fisheye lens, with 11 participants noting that it was easy to determine the location of the target when using the fisheye lens. P10 remarked, *"The fisheye lens had no blind spots, so it was easy to find the red target."* However, the unique motion of targets on the fisheye lens contributed to the difficulty in operating it. P1 remarked, *"It is more difficult to display the target at the center of the lens compared to the linear lens."*

5.7.3 Lens Position. Most participants left positive comments about the Center condition. Eight participants noted that the Center condition was easier to use than the Upper-Right condition, regardless of the *Lens Type*. P4 remarked, *"The Center condition makes it easier to understand the relationship between the target and the lens positions."* On the other hand, some participants left negative comments about the Upper-Right condition. They (P5, P8, P9, P11, P22) commented that the Upper-Right condition imposed a high physical burden. Additional issues mentioned included eye fatigue (P5) and difficulty in selecting lower-positioned targets (P9, P11). These comments suggest that participants tended to prefer the Center condition over the Upper-Right condition due to its ease and comfort in selecting targets.

5.7.4 Activation Gesture. Participants expressed their dissatisfaction with the activation gesture. Nine participants commented that it was burdensome to repeatedly and continuously activate the magnifier by dwelling the gaze on the upper-right position. Additionally, some participants reported difficulty with the gesture (P14, P22) and eye fatigue (P6, P17, P20, P21).

5.8 Summary of the Study

We summarize the study result in Table 2. The fisheye lens demonstrated significantly better performance than the linear lens in terms of error rate, target search time, and total target selection time. On the other hand, the linear lens exhibited a significantly faster target selection time compared to the fisheye lens.

For *Lens Position*, the Center condition showed significantly better performance in terms of error rate, target selection time, total target selection time, SUS, and NASA-TLX scores. Notably, in the FC and LC conditions, participants were able to select 1° objects, which is too small to select using a standard gaze interface, with significantly lower error rates (3.37% and 2.38%, respectively).

For *Lens Width*, larger *Lens Width* values resulted in better error rates for LU, FC, and FU. Additionally, a larger *Lens Width* improved the target selection time for FU. In contrast, smaller *Lens Width* values led to lower error rates and total selection time for LC, as well as improved target search time for LU.

6 Discussion

We conducted the user study to investigate whether our method can make it easy to select small targets in the condition combined *Lens Type* and *Lens Positoin*. We discuss the selection performance of GazeScope, the activation gesture, comparisons with existing methods, and the limitations of this research.

6.1 Selection Performance and Usability of GazeScope

The user study results demonstrate that GazeScope can facilitate the selection of small targets. In particular, in the Center condition, participants were able to accurately select significantly small targets (*Target Width* = 1°) with an error rate of 2.88%. Therefore, GazeScope is an effective method for selecting small targets in VR environments.

On the other hand, the total selection time for GazeScope was relatively long, even in the FC condition, where the fastest total selection time was 3.73 s. This is because selecting a target with GazeScope involves three steps: activating the magnifier, capturing the target within the magnifier, and selecting the target inside the magnifier. Nevertheless, GazeScope enables a highly accurate selection of small objects. Therefore, GazeScope is better suited for scenarios where selection accuracy is prioritized over speed or when selecting targets that cannot be accessed using conventional dwell time selection methods.

The SUS results showed that the FC condition achieved a high usability score, suggesting that GazeScope, when appropriately designed, offers better usability. However, based on participants' feedback, many expressed dissatisfaction with the magnifier activation gesture. This dissatisfaction stemmed from the gesture requiring larger eye movements than usual. In this study, participants performed 252 gestures (or more, including practice), which led to eye fatigue. However, since this gesture is only performed when the user chooses to activate the magnifier, its frequency of use is expected to be lower in real-world scenarios. Therefore, we believe that the burden of the magnifier activation gesture would not pose a significant issue in practical use.

6.2 Appropriate Parameters

The study results indicate that *Lens Position* had the most significant impact on GazeScope's selection performance. The Center condition showed significantly better selection performance compared to the Upper-Right condition. As shown in Table 2, LC or FC performed the best in six categories. This suggests that displaying the magnifier at the gaze position when the magnifier activation gesture is performed is not suitable for our method, which utilizes an area of 25° from the head direction.

In terms of *Lens Type*, the fisheye lens received more positive comments from participants than the linear lens. Unlike the linear lens, the fisheye lens has no blind spots, which makes it superior in terms of target search time. Some participants provided negative feedback regarding the linear lens, noting that the target became invisible. Due to this occlusion, some participants preferred a smaller lens width for linear lenses. Thus, the occlusion caused by linear lenses negatively impacts the user experience. On the other hand, the fisheye lens was inferior to the linear lens in terms of target selection time. This is due to the additional time required to move the target into the area of the magnifier where linear magnification is applied (near the center of the fisheye lens).

Regarding *Lens Width*, fisheye lenses with a larger lens width demonstrated superior performance. This is because the area expanded using a fisheye lens increases as the lens width becomes larger, making it easier to select smaller targets. In contrast, for

Table 2: Table of performance metrics for each *Lens Type* × *Lens Position* condition (LC, LU, FC, FU). The top two values for each metric are highlighted, with the best values shown in dark green and the second-best values in light green. Roman numerals represent the ranking for each metric.

	Error Rate (%)	Target Search Time (s)	Target Selection Time (s)	Total Selection Time (s)	SUS	NASA-TLX
LC	II: 2.31 ± 7.75	IV: 1.52 ± 0.93	I: 1.02 ± 0.57	II: 4.03 ± 1.41	II: 73.54 ± 19.07	II: 44.44 ± 20.65
LU	III: 4.70 ± 11.76	III: 1.47 ± 0.98	III: 1.29 ± 0.99	IV: 4.21 ± 1.55	IV: 56.04 ± 20.99	III: 53.51 ± 20.60
FC	I: 1.12 ± 5.48	I: 1.11 ± 0.50	II: 1.12 ± 0.79	I: 3.73 ± 1.23	I: 77.50 ± 20.63	I: 38.40 ± 22.94
FU	IV: 5.82 ± 13.71	II: 1.18 ± 0.89	IV: 1.64 ± 1.40	III: 4.19 ± 1.70	III: 57.60 ± 21.56	IV: 55.03 ± 21.41

linear lenses, particularly LC, a smaller lens width resulted in better error rates and shorter total selection time. This is because a smaller lens width reduces the area obscured by the magnifier, facilitating easier target capture within the magnified region. Therefore, a smaller lens width is preferable when using a linear lens as a magnifying tool for GazeScope. Conversely, a larger lens width is recommended when using a fisheye lens.

6.3 Comparison with Existing Methods for Small Object Selection

GazeScope achieves higher accuracy in selecting small targets than existing methods. According to the study results, the error rate for FC was 1.12%, while the error rate for FC when selecting a 1° target was 2.38%. This error rate is lower than those of other methods that use eye and head input [59, 60, 64]. Additionally, the error rate is sufficiently low compared to methods that use hand input [4, 9, 78]. This is because dwell time input eliminates the possibility of "selecting outside the target" errors [48], resulting in a lower error rate than those methods. Notably, direct comparisons of error rates should be interpreted with caution due to differences in experimental conditions. However, our proposed method can be considered highly accurate in selecting small objects.

On the other hand, the total selection time for GazeScope, at 3.73 s, is significantly longer than that of other methods. The selection time for Cone&Bubble [64], which uses both gaze and head input, ranges from 1.5 s to 2.0 s, making it much faster than GazeScope. Additionally, studies on methods that utilize other modalities have also reported faster selection times than GazeScope [4, 8, 71]. Thus, GazeScope is less efficient than existing methods in terms of selection time.

The key contribution of GazeScope is that it enables the use of a magnifier in 3D environments hands-free. Approaches for selecting small or occluded objects, such as removing occlusions [9, 43, 78], generating different viewpoints[41, 80], and repositioning [7, 13, 22, 36, 54, 78], can only be applied to virtual objects and not real ones. Although a magnifier cannot eliminate a target's occlusion, it can magnify small real objects. Additionally, a magnifier can be used to expand the FOV in everyday life. We believe that GazeScope is advantageous because it allows individuals who have difficulty using their hands or whose hands are occupied to utilize a magnifier in 3D environments.

6.4 Limitations

Our research has several limitations. First, our research did not compare GazeScope with previous methods and instead focused solely on the design parameters of GazeScope. Due to the lack of prior knowledge about implementing a magnifier as a gaze interface in a VR environment, it was necessary to investigate parameters related to magnifiers. Now that our study has identified the appropriate magnifier parameters for GazeScope, it should be compared with previous methods in future research.

Second, the study of GazeScope's magnifier activation gestures is insufficient. Since we have only implemented a single magnifier activation gesture, it remains unclear whether this gesture is superior to other potential gestures (e.g., blink, wink). Therefore, further research is required to compare and evaluate alternative input gestures for the magnifier activation.

Third, the functions necessary for the practical use of GazeScope, such as closing the magnifier and adjusting the magnification rate, have not been investigated. Although these functions are essential [58], they were not considered in this study. These functions can be implemented by placing menu items around the magnifier [63] or using gaze gestures toward its edge [28, 29]. Therefore, developing and evaluating practical functionalities for GazeScope is necessary.

Finally, this study has limitations related to the participants and study tasks. Most participants were young male university students, leading to a narrow range of age and gender. Additionally, although we conducted a controlled target selection task to examine the parameters of an appropriate magnifier for GazeScope, its selection performance in scenarios such as selecting occluded objects or performing tasks requiring visual search remains unclear. Moreover, we did not explicitly evaluate selection errors caused by head rotations, leaving the potential impact of such errors on target selection unexamined. Future research should investigate how head movements affect GazeScope's performance and accuracy. Furthermore, this study did not focus on selecting real-world objects in an AR environment. Therefore, additional research is required to evaluate the selection performance of GazeScope across various objects and environments.

7 Conclusion

We presented GazeScope, a method for selecting small targets using gaze and head input in VR environments. Our method allows the magnifier to be activated solely through gaze input. We examined whether GazeScope could facilitate the selection of small targets and identified appropriate parameters for the magnifier. The results showed that GazeScope achieved an error rate of 2.9% when selecting small targets, and displaying the magnifier in the direction of the user's head further improved selection performance. Our method enables the user to effectively select small targets by activating the magnifier in a VR environment, significantly expanding the potential applications of gaze interfaces.

Acknowledgments

This work was partially supported by JSPS KAKENHI Grant Numbers 24K21319 and 23K21684.

References

[1] Sondre Agledahl and Anthony Steed. 2021. Magnification Vision – a Novel Gaze-Directed User Interface. In *2021 IEEE Conference on Virtual Reality and 3D User Interfaces Abstracts and Workshops (VRW)*. 474–475. https://doi.org/10.1109/VRW52623.2021.00119

[2] Caroline Appert, Olivier Chapuis, and Emmanuel Pietriga. 2010. High-Precision Magnification Lenses. In *Proceedings of the SIGCHI Conference on Human Factors in Computing Systems* (Atlanta, Georgia, USA) *(CHI '10)*. Association for Computing Machinery, New York, NY, USA, 273–282. https://doi.org/10.1145/1753326.1753366

[3] Michael Ashmore, Andrew T. Duchowski, and Garth Shoemaker. 2005. Efficient Eye Pointing with a Fisheye Lens. In *Proceedings of Graphics Interface 2005* (Victoria, British Columbia) *(GI '05)*. Canadian Human-Computer Communications Society, School of Computer Science, University of Waterloo, Waterloo, Ontario, Canada, 203–210. http://dl.acm.org/citation.cfm?id=1089508.1089542

[4] Marc Baloup, Thomas Pietrzak, and Géry Casiez. 2019. RayCursor: A 3D Pointing Facilitation Technique based on Raycasting. In *Proceedings of the 2019 CHI Conference on Human Factors in Computing Systems* (Glasgow, Scotland Uk) *(CHI '19)*. Association for Computing Machinery, New York, NY, USA, 1–12. https://doi.org/10.1145/3290605.3300331

[5] Richard Bates and Howell Istance. 2002. Zooming Interfaces!: Enhancing the Performance of Eye Controlled Pointing Devices. In *Proceedings of the Fifth International ACM Conference on Assistive Technologies* (Edinburgh, Scotland) *(Assets '02)*. ACM, New York, NY, USA, 119–126. https://doi.org/10.1145/638249.638272

[6] John Brooke. 1995. SUS: A quick and dirty usability scale. *Usability Eval. Ind.* 189 (1995).

[7] Jeffrey Cashion, Chadwick Wingrave, and Joseph J. LaViola Jr. 2012. Dense and Dynamic 3D Selection for Game-Based Virtual Environments. *IEEE Transactions on Visualization and Computer Graphics* 18, 4 (2012), 634–642. https://doi.org/10.1109/TVCG.2012.40

[8] Di Laura Chen, Marcello Giordano, Hrvoje Benko, Tovi Grossman, and Stephanie Santosa. 2023. GazeRayCursor: Facilitating Virtual Reality Target Selection by Blending Gaze and Controller Raycasting. In *Proceedings of the 29th ACM Symposium on Virtual Reality Software and Technology* (Christchurch, New Zealand) *(VRST '23)*. Association for Computing Machinery, New York, NY, USA, Article 19, 11 pages. https://doi.org/10.1145/3611659.3615693

[9] Yuan Chen, Junwei Sun, Qiang Xu, Edward Lank, Pourang Irani, and Wei Li. 2021. Global Scene Filtering, Exploration, and Pointing in Occluded Virtual Space. In *Human-Computer Interaction – INTERACT 2021: 18th IFIP TC 13 International Conference, Bari, Italy, August 30 – September 3, 2021, Proceedings, Part V* (Bari, Italy). Springer-Verlag, Berlin, Heidelberg, 156–176. https://doi.org/10.1007/978-3-030-85607-6_11

[10] Myungguen Choi, Daisuke Sakamoto, and Tetsuo Ono. 2020. Bubble Gaze Cursor + Bubble Gaze Lens: Applying Area Cursor Technique to Eye-Gaze Interface. In *ACM Symposium on Eye Tracking Research and Applications* (Stuttgart, Germany) *(ETRA '20 Full Papers)*. Association for Computing Machinery, New York, NY, USA, Article 11, 10 pages. https://doi.org/10.1145/3379155.3391322

[11] Myungguen Choi, Daisuke Sakamoto, and Tetsuo Ono. 2022. Kuiper Belt: Utilizing the "Out-of-Natural Angle" Region in the Eye-Gaze Interaction for Virtual Reality. In *Proceedings of the 2022 CHI Conference on Human Factors in Computing Systems* (New Orleans, LA, USA) *(CHI '22)*. Association for Computing Machinery, New York, NY, USA, Article 357, 17 pages. https://doi.org/10.1145/3491102.3517725

[12] Nathan Cournia, John D. Smith, and Andrew T. Duchowski. 2003. Gaze- vs. Hand-Based Pointing in Virtual Environments. In *CHI '03 Extended Abstracts on Human Factors in Computing Systems* (Ft. Lauderdale, Florida, USA) *(CHI EA '03)*. Association for Computing Machinery, New York, NY, USA, 772–773. https://doi.org/10.1145/765891.765982

[13] Henrique Debarba, Jeronimo Grandi, Anderson Maciel, Luciana Nedel, and Ronan Boulic. 2013. Disambiguation Canvas: A Precise Selection Technique for Virtual Environments. In *Human-Computer Interaction – INTERACT 2013*. Springer Berlin Heidelberg, Berlin, Heidelberg, 388–405.

[14] Shujie Deng, Jian Chang, Shi-Min Hu, and Jian Jun Zhang. 2017. Gaze Modulated Disambiguation Technique for Gesture Control in 3D Virtual Objects Selection. In *2017 3rd IEEE International Conference on Cybernetics (CYBCONF)*. 1–8. https://doi.org/10.1109/CYBConf.2017.7985779

[15] Lisa A. Elkin, Matthew Kay, James J. Higgins, and Jacob O. Wobbrock. 2021. An Aligned Rank Transform Procedure for Multifactor Contrast Tests. In *The 34th Annual ACM Symposium on User Interface Software and Technology* (Virtual Event, USA) *(UIST '21)*. Association for Computing Machinery, New York, NY, USA, 754–768. https://doi.org/10.1145/3472749.3474784

[16] Anna Maria Feit, Shane Williams, Arturo Toledo, Ann Paradiso, Harish Kulkarni, Shaun Kane, and Meredith Ringel Morris. 2017. Toward Everyday Gaze Input: Accuracy and Precision of Eye Tracking and Implications for Design. In *Proceedings of the 2017 CHI Conference on Human Factors in Computing Systems* (Denver, Colorado, USA) *(CHI '17)*. Association for Computing Machinery, New York, NY, USA, 1118–1130. https://doi.org/10.1145/3025453.3025599

[17] S Fortune. 1986. A sweepline algorithm for Voronoi diagrams. In *Proceedings of the Second Annual Symposium on Computational Geometry* (Yorktown Heights, New York, USA) *(SCG '86)*. Association for Computing Machinery, New York, NY, USA, 313–322. https://doi.org/10.1145/10515.10549

[18] Tom Foulsham, Esther Walker, and Alan Kingstone. 2011. To Where, What and When of Gaze Allocation in the Lab and the Natural Environment. *Vision research* 51 (2011), 1920–1931. https://doi.org/10.1016/j.visres.2011.07.002

[19] Julie Fraser and Carl Gutwin. 2000. A framework of assistive pointers for low vision users. In *Proceedings of the Fourth International ACM Conference on Assistive Technologies* (Arlington, Virginia, USA) *(Assets '00, 8)*. Association for Computing Machinery, New York, NY, USA, 9–16. https://doi.org/10.1145/354324.354329

[20] G. W. Furnas. 1986. Generalized Fisheye Views. In *Proceedings of the SIGCHI Conference on Human Factors in Computing Systems* (Boston, Massachusetts, USA) *(CHI '86)*. Association for Computing Machinery, New York, NY, USA, 16—-23. https://doi.org/10.1145/22627.22342

[21] Tovi Grossman and Ravin Balakrishnan. 2005. The bubble cursor: enhancing target acquisition by dynamic resizing of the cursor's activation area. In *Proceedings of the SIGCHI Conference on Human Factors in Computing Systems* (Portland, Oregon, USA) *(CHI '05)*. Association for Computing Machinery, New York, NY, USA, 281–290. https://doi.org/10.1145/1054972.1055012

[22] Tovi Grossman and Ravin Balakrishnan. 2006. The Design and Evaluation of Selection Techniques for 3D Volumetric Displays. In *Proceedings of the 19th Annual ACM Symposium on User Interface Software and Technology* (Montreux, Switzerland) *(UIST '06)*. Association for Computing Machinery, New York, NY, USA, 3–12. https://doi.org/10.1145/1166253.1166257

[23] Carl Gutwin. 2002. Improving Focus Targeting in Interactive Fisheye Views. In *Proceedings of the SIGCHI Conference on Human Factors in Computing Systems* (Minneapolis, Minnesota, USA) *(CHI '02)*. Association for Computing Machinery, New York, NY, USA, 267–274. https://doi.org/10.1145/503376.503424

[24] Sandra G. Hart and Lowell E. Staveland. 1988. Development of NASA-TLX (Task Load Index): Results of Empirical and Theoretical Research. In *Human Mental Workload*, Peter A. Hancock and Najmedin Meshkati (Eds.). Advances in Psychology, Vol. 52. North-Holland, Netherlands, 139–183. https://doi.org/10.1016/S0166-4115(08)62386-9

[25] James J. Higgins and Suleiman Tashtoush. 1994. An aligned rank transform test for interaction. *Nonlinear World* 1, 2 (1994), 201–211.

[26] Sture Holm. 1979. A Simple Sequentially Rejective Multiple Test Procedure. *Scandinavian Journal of Statistics* 6, 2 (1979), 65–70.

[27] Zhiming Hu, Sheng Li, Congyi Zhang, Kangrui Yi, Guoping Wang, and Dinesh Manocha. 2020. DGaze: CNN-Based Gaze Prediction in Dynamic Scenes. *IEEE Transactions on Visualization and Computer Graphics* 26, 5 (2020), 1902–1911.

[28] Poika Isokoski. 2000. Text input methods for eye trackers using off-screen targets. In *Proceedings of the 2000 Symposium on Eye Tracking Research & Applications* (Palm Beach Gardens, Florida, USA) *(ETRA '00)*. Association for Computing Machinery, New York, NY, USA, 15–21. https://doi.org/10.1145/355017.355020

[29] Howell Istance, Aulikki Hyrskykari, Lauri Immonen, Santtu Mansikkamaa, and Stephen Vickers. 2010. Designing gaze gestures for gaming: an investigation of performance. In *Proceedings of the 2010 Symposium on Eye-Tracking Research & Applications* (Austin, Texas) *(ETRA '10)*. Association for Computing Machinery, New York, NY, USA, 323–330. https://doi.org/10.1145/1743666.1743740

[30] Robert J. K. Jacob. 1990. What You Look at is What You Get: Eye Movement-Based Interaction Techniques. In *Proceedings of the SIGCHI Conference on Human Factors in Computing Systems* (Seattle, Washington, USA) *(CHI '90)*. Association for Computing Machinery, New York, NY, USA, 11–18. https://doi.org/10.1145/97243.97246

[31] Jorge Jimenez, Diego Gutierrez, and Pedro Latorre. 2008. Gaze-based Interaction for Virtual Environments. *Journal of Universal Computer Science* 14, 19 (2008), 3085–3098.

[32] T.A. Keahey and E.L. Robertson. 1996. Techniques for non-linear magnification transformations. In *Proceedings IEEE Symposium on Information Visualization '96*. 38–45. https://doi.org/10.1109/INFVIS.1996.559214

[33] Mohamed Khamis, Carl Oechsner, Florian Alt, and Andreas Bulling. 2018. VR-pursuits: Interaction in Virtual Reality Using Smooth Pursuit Eye Movements.

In *Proceedings of the 2018 International Conference on Advanced Visual Interfaces* (Castiglione della Pescaia, Grosseto, Italy) *(AVI '18)*. Association for Computing Machinery, New York, NY, USA, Article 18, 8 pages. https://doi.org/10.1145/3206505.3206522

[34] Konstantin Klamka, Andreas Siegel, Stefan Vogt, Fabian Göbel, Sophie Stellmach, and Raimund Dachselt. 2015. Look & Pedal: Hands-free Navigation in Zoomable Information Spaces Through Gaze-supported Foot Input. In *Proceedings of the 2015 ACM on International Conference on Multimodal Interaction* (Seattle, Washington, USA) *(ICMI '15)*. ACM, New York, NY, USA, 123–130. https://doi.org/10.1145/2818346.2820751

[35] Richard L. Kline and Ephraim P. Glinert. 1995. Improving GUI accessibility for people with low vision. In *Proceedings of the SIGCHI Conference on Human Factors in Computing Systems* (Denver, Colorado, USA) *(CHI '95, 8)*. ACM Press/Addison-Wesley Publishing Co., USA, 114–121. https://doi.org/10.1145/223904.223919

[36] Regis Kopper, Felipe Bacim, and Doug Bowman. 2011. Rapid and accurate 3D selection by progressive refinement. In *2011 IEEE Symposium on 3D User Interfaces (3DUI)* (Singapore). IEEE, USA, 67–74. https://doi.org/10.1109/3DUI.2011.5759219

[37] Manu Kumar, Andreas Paepcke, Terry Winograd, and Terry Winograd. 2007. EyePoint: Practical Pointing and Selection Using Gaze and Keyboard. In *Proceedings of the SIGCHI Conference on Human Factors in Computing Systems* (San Jose, California, USA) *(CHI '07)*. ACM, New York, NY, USA, 421–430. https://doi.org/10.1145/1240624.1240692

[38] Mikko Kytö, Barrett Ens, Thammathip Piumsomboon, Gun A. Lee, and Mark Billinghurst. 2018. Pinpointing: Precise Head- and Eye-Based Target Selection for Augmented Reality. In *Proceedings of the 2018 CHI Conference on Human Factors in Computing Systems* (Montreal QC, Canada) *(CHI '18)*. Association for Computing Machinery, New York, NY, USA, 1–14. https://doi.org/10.1145/3173574.3173655

[39] Chris Lankford. 2000. Effective Eye-gaze Input into Windows. In *Proceedings of the 2000 Symposium on Eye Tracking Research & Applications* (Palm Beach Gardens, Florida, USA) *(ETRA '00)*. ACM, New York, NY, USA, 23–27. https://doi.org/10.1145/355017.355021

[40] Geonsun Lee, Jennifer Healey, and Dinesh Manocha. 2022. VRDoc: Gaze-based Interactions for VR Reading Experience. In *2022 IEEE International Symposium on Mixed and Augmented Reality (ISMAR)*. 787–796. https://doi.org/10.1109/ISMAR55827.2022.00097

[41] Nianlong Li, Zhengquan Zhang, Can Liu, Zengyao Yang, Yinan Fu, Feng Tian, Teng Han, and Mingming Fan. 2021. vMirror: Enhancing the Interaction with Occluded or Distant Objects in VR with Virtual Mirrors. In *Proceedings of the 2021 CHI Conference on Human Factors in Computing Systems* (Yokohama, Japan) *(CHI '21)*. Association for Computing Machinery, New York, NY, USA, Article 132, 11 pages. https://doi.org/10.1145/3411764.3445537

[42] Yiqin Lu, Chun Yu, and Yuanchun Shi. 2020. Investigating Bubble Mechanism for Ray-Casting to Improve 3D Target Acquisition in Virtual Reality. In *2020 IEEE Conference on Virtual Reality and 3D User Interfaces (VR)*. 35–43. https://doi.org/10.1109/VR46266.2020.00021

[43] Jiaju Ma, Jing Qian, Tongyu Zhou, and Jeff Huang. 2023. FocalPoint: Adaptive Direct Manipulation for Selecting Small 3D Virtual Objects. *Proc. ACM Interact. Mob. Wearable Ubiquitous Technol.* 7, 1, Article 22 (2023), 26 pages. https://doi.org/10.1145/3580856

[44] Diako Mardanbegi, Benedikt Mayer, Ken Pfeuffer, Shahram Jalaliniya, Hans Gellersen, and Alexander Perzl. 2019. EyeSeeThrough: Unifying Tool Selection and Application in Virtual Environments. In *2019 IEEE Conference on Virtual Reality and 3D User Interfaces (VR)*. 474–483. https://doi.org/10.1109/VR.2019.8797988

[45] Sina Masnadi, Brian Williamson, Andrés N. Vargas González, and Joseph J. LaViola. 2020. VRiAssist: An Eye-Tracked Virtual Reality Low Vision Assistance Tool. In *2020 IEEE Conference on Virtual Reality and 3D User Interfaces Abstracts and Workshops (VRW)*. 808–809. https://doi.org/10.1109/VRW50115.2020.00255

[46] Pedro Monteiro, Guilherme Gonçalves, Bruno Peixoto, Miguel Melo, and Maximino Bessa. 2023. Evaluation of Hands-Free VR Interaction Methods During a Fitts' Task: Efficiency and Effectiveness. *IEEE Access* 11 (2023), 70898–70911. https://doi.org/10.1109/ACCESS.2023.3293057

[47] Aunnoy Mutasim, Anil Ufuk Batmaz, Moaaz Hudhud Mughrabi, and Wolfgang Stuerzlinger. 2022. Performance Analysis of Saccades for Primary and Confirmatory Target Selection. In *Proceedings of the 28th ACM Symposium on Virtual Reality Software and Technology* (Tsukuba, Japan) *(VRST '22)*. Association for Computing Machinery, New York, NY, USA, Article 18, 12 pages. https://doi.org/10.1145/3562939.3565619

[48] Aunnoy K Mutasim, Anil Ufuk Batmaz, and Wolfgang Stuerzlinger. 2021. Pinch, Click, or Dwell: Comparing Different Selection Techniques for Eye-Gaze-Based Pointing in Virtual Reality. In *ACM Symposium on Eye Tracking Research and Applications* (Virtual Event, Germany) *(ETRA '21 Short Papers)*. Association for Computing Machinery, New York, NY, USA, Article 15, 7 pages. https://doi.org/10.1145/3448018.3457998

[49] L. Jacob Orquin and Kenneth Holmqvist. 2017. Threats to the Validity of Eye-Movement Research in Psychology. *Behavior Research Methods* 50 (2017). https://doi.org/10.3758/s13428-017-0998-z

[50] Ken Pfeuffer, Yasmeen Abdrabou, Augusto Esteves, Radiah Rivu, Yomna Abdelrahman, Stefanie Meitner, Amr Saadi, and Florian Alt. 2021. ARtention: A design space for gaze-adaptive user interfaces in augmented reality. *Computers & Graphics* 95 (2021), 1–12. https://doi.org/10.1016/j.cag.2021.01.001

[51] Ken Pfeuffer and Hans Gellersen. 2016. Gaze and Touch Interaction on Tablets. In *Proceedings of the 29th Annual Symposium on User Interface Software and Technology* (Tokyo, Japan) *(UIST '16)*. Association for Computing Machinery, New York, NY, USA, 301–311. https://doi.org/10.1145/2984511.2984514

[52] Thammathip Piumsomboon, Gun Lee, Robert W. Lindeman, and Mark Billinghurst. 2017. Exploring natural eye-gaze-based interaction for immersive virtual reality. In *2017 IEEE Symposium on 3D User Interfaces (3DUI) (3DUI '17)*. IEEE, USA, 36–39. https://doi.org/10.1109/3DUI.2017.7893315

[53] Carole Plasson, Dominique Cunin, Yann Laurillau, and Laurence Nigay. 2021. A Lens-Based Extension of Raycasting for Accurate Selection in Dense 3D Environments. In *Human-Computer Interaction – INTERACT 2021: 18th IFIP TC 13 International Conference, Bari, Italy, August 30 – September 3, 2021, Proceedings, Part IV* (Bari, Italy). Springer-Verlag, Berlin, Heidelberg, 501–524. https://doi.org/10.1007/978-3-030-85610-6_28

[54] Gang Ren and Eamonn O'Neill. 2012. 3D selection with freehand gesture. *Computers & Graphics* 37, 3 (2012), 101–120. https://doi.org/10.1016/j.cag.2012.12.006

[55] K. C. Salter and R. F Fawcett. 1993. The art test of interaction: a robust and powerful rank test of interaction in factorial models. *Communications in Statistics - Simulation and Computation* 22, 1 (1993), 137–153. https://doi.org/10.1080/03610919308813085

[56] Florian Schniederjann, Jana Krahe, Tobias Guth, Johanna Wendel, and Robert Mertens. 2018. Using Linear and Non-linear Magnifiers in Eyetracking-Based Human Computer Interaction. In *2018 IEEE International Symposium on Multimedia (ISM)*. 190–191. https://doi.org/10.1109/ISM.2018.00-10

[57] Florian Schniederjann, Darius Rausch, Jens Wiggenbrock, and Robert Mertens. 2022. Teardrop Magnification: A Hybrid Linear-Fisheye Magnifier for the Border and Corner of the Screen. In *2022 IEEE International Symposium on Multimedia (ISM)*. 82–83. https://doi.org/10.1109/ISM55400.2022.00017

[58] Ryan Schubert, Gerd Bruder, and Greg Welch. 2023. Intuitive User Interfaces for Real-Time Magnification in Augmented Reality. In *Proceedings of the 29th ACM Symposium on Virtual Reality Software and Technology* (Christchurch, New Zealand) *(VRST '23)*. Association for Computing Machinery, New York, NY, USA, Article 12, 10 pages. https://doi.org/10.1145/3611659.3615694

[59] Ludwig Sidenmark, Christopher Clarke, Joshua Newn, Mathias N. Lystbæk, Ken Pfeufer, and Hans Gellersen. 2023. Vergence Matching: Inferring Attention to Objects in 3D Environments for Gaze-Assisted Selection *(CHI '23)*. Association for Computing Machinery, New York, NY, USA, 1–15. https://doi.org/10.1145/3544548.3580685

[60] Ludwig Sidenmark, Christopher Clarke, Xuesong Zhang, Jenny Phu, and Hans Gellersen. 2020. Outline Pursuits: Gaze-assisted Selection of Occluded Objects in Virtual Reality. In *Proceedings of the 2020 CHI Conference on Human Factors in Computing Systems* (Honolulu, HI, USA) *(CHI '20)*. Association for Computing Machinery, New York, NY, USA, 1–13. https://doi.org/10.1145/3313831.3376438

[61] Ludwig Sidenmark and Hans Gellersen. 2019. Eye & Head: Synergetic Eye and Head Movement for Gaze Pointing and Selection. In *Proceedings of the 32nd Annual ACM Symposium on User Interface Software and Technology* (New Orleans, LA, USA) *(UIST '19)*. Association for Computing Machinery, New York, NY, USA, 1161–1174. https://doi.org/10.1145/3332165.3347921

[62] Ludwig Sidenmark and Hans Gellersen. 2019. Eye, Head and Torso Coordination During Gaze Shifts in Virtual Reality. *ACM Transactions on Computer-Human Interaction (TOCHI)* 27, 1, Article 4 (2019), 40 pages. https://doi.org/10.1145/3361218

[63] Ludwig Sidenmark, Dominic Potts, Bill Bapisch, and Hans Gellersen. 2021. Radi-Eye: Hands-Free Radial Interfaces for 3D Interaction Using Gaze-Activated Head-Crossing. In *Proceedings of the 2021 CHI Conference on Human Factors in Computing Systems* (Yokohama, Japan) *(CHI '21)*. Association for Computing Machinery, New York, NY, USA, Article 740, 11 pages. https://doi.org/10.1145/3411764.3445697

[64] Ludwig Sidenmark, Zibo Sun, and Hans Gellersen. 2024. Cone&Bubble: Evaluating Combinations of Gaze, Head and Hand Pointing for Target Selection in Dense 3D Environments. In *2024 IEEE Conference on Virtual Reality and 3D User Interfaces Abstracts and Workshops (VRW)*. 642–649. https://doi.org/10.1109/VRW62533.2024.00126

[65] John Stahl. 2001. Eye-Head Coordination and the Variation of Eye-Movement Accuracy with Orbital Eccentricity. *Experimental brain research. Experimentelle Hirnforschung. Expérimentation cérébrale* 136 (2001), 200–210. https://doi.org/10.1007/s002210000593

[66] Sophie Stellmach and Raimund Dachselt. 2012. Look & touch: gaze-supported target acquisition. In *Proceedings of the SIGCHI Conference on Human Factors in Computing Systems* (Austin, Texas, USA) *(CHI '12)*. Association for Computing Machinery, New York, NY, USA, 2981–2990. https://doi.org/10.1145/2207676.2208709

[67] Sophie Stellmach and Raimund Dachselt. 2013. Still looking: investigating seamless gaze-supported selection, positioning, and manipulation of distant targets.

In *Proceedings of the SIGCHI Conference on Human Factors in Computing Systems* (Paris, France) *(CHI '13)*. Association for Computing Machinery, New York, NY, USA, 285–294. https://doi.org/10.1145/2470654.2470695

[68] Sophie Stellmach, Sebastian Stober, Andreas Nürnberger, and Raimund Dachselt. 2011. Designing gaze-supported multimodal interactions for the exploration of large image collections. In *Proceedings of the 1st Conference on Novel Gaze-Controlled Applications* (Karlskrona, Sweden) *(NGCA '11)*. Association for Computing Machinery, New York, NY, USA, Article 1, 8 pages. https://doi.org/10.1145/1983302.1983303

[69] Meini Tang, Roberto Manduchi, Susana Chung, and Raquel Prado. 2023. Screen Magnification for Readers with Low Vision: A Study on Usability and Performance. In *Proceedings of the 25th International ACM SIGACCESS Conference on Computers and Accessibility* (New York, NY, USA) *(ASSETS '23, 23)*. Association for Computing Machinery, New York, NY, USA, 1–15. https://doi.org/10.1145/3597638.3608383

[70] Vildan Tanriverdi and Robert J. K. Jacob. 2000. Interacting with Eye Movements in Virtual Environments. In *Proceedings of the SIGCHI Conference on Human Factors in Computing Systems* (The Hague, The Netherlands) *(CHI '00)*. Association for Computing Machinery, New York, NY, USA, 265–272. https://doi.org/10.1145/332040.332443

[71] Yang Tian, Yulin Zheng, Shengdong Zhao, Xiaojuan Ma, and Yunhai Wang. 2023. Balancing Accuracy and Speed in Gaze-Touch Grid Menu Selection in AR via Mapping Sub-Menus to a Hand-Held Device. *Sensors* 23, 23 (2023). https://doi.org/10.3390/s23239587

[72] Lode Vanacken, Tovi Grossman, and Karin Coninx. 2007. Exploring the Effects of Environment Density and Target Visibility on Object Selection in 3D Virtual Environments. In *2007 IEEE Symposium on 3D User Interfaces*. https://doi.org/10.1109/3DUI.2007.340783

[73] Uta Wagner, Matthias Albrecht, Andreas Asferg Jacobsen, Haopeng Wang, Hans Gellersen, and Ken Pfeuffer. 2024. Gaze, Wall, and Racket: Combining Gaze and Hand-Controlled Plane for 3D Selection in Virtual Reality. *Proceedings of the ACM on Human-Computer Interaction.* 8, ISS, Article 534 (2024), 25 pages. https://doi.org/10.1145/3698134

[74] Ru Wang, Zach Potter, Yun Ho, Daniel Killough, Linxiu Zeng, Sanbrita Mondal, and Yuhang Zhao. 2024. GazePrompt: Enhancing Low Vision People's Reading Experience with Gaze-Aware Augmentations. In *Proceedings of the 2024 CHI Conference on Human Factors in Computing Systems* (Honolulu, HI, USA) *(CHI '24)*. Association for Computing Machinery, New York, NY, USA, Article 894, 17 pages. https://doi.org/10.1145/3613904.3642878

[75] Jacob O. Wobbrock, Leah Findlater, Darren Gergle, and James J. Higgins. 2011. The Aligned Rank Transform for Nonparametric Factorial Analyses Using Only Anova Procedures. In *Proceedings of the SIGCHI Conference on Human Factors in Computing Systems* (Vancouver, BC, Canada) *(CHI '11)*. Association for Computing Machinery, New York, NY, USA, 143–146. https://doi.org/10.1145/1978942.1978963

[76] Xin Yi, Yiqin Lu, Ziyin Cai, Zihan Wu, Yuntao Wang, and Yuanchun Shi. 2022. GazeDock: Gaze-Only Menu Selection in Virtual Reality using Auto-Triggering Peripheral Menu. In *2022 IEEE Conference on Virtual Reality and 3D User Interfaces (VR)*. 832–842. https://doi.org/10.1109/VR51125.2022.00105

[77] Xin Yi, Leping Qiu, Wenjing Tang, Yehan Fan, Hewu Li, and Yuanchun Shi. 2022. DEEP: 3D Gaze Pointing in Virtual Reality Leveraging Eyelid Movement. In *Proceedings of the 35th Annual ACM Symposium on User Interface Software and Technology* (Bend, OR, USA) *(UIST '22)*. Association for Computing Machinery, New York, NY, USA, Article 3, 14 pages. https://doi.org/10.1145/3526113.3545673

[78] Difeng Yu, Qiushi Zhou, Joshua Newn, Tilman Dingler, Eduardo Velloso, and Jorge Goncalves. 2020. Fully-Occluded Target Selection in Virtual Reality. *IEEE Transactions on Visualization and Computer Graphics* 26, 12 (2020), 3402–3413. https://doi.org/10.1109/TVCG.2020.3023606

[79] Xinyong Zhang, Pianpian Xu, Qing Zhang, and Hongbin Zha. 2011. Speed-Accuracy Trade-off in Dwell-Based Eye Pointing Tasks at Different Cognitive Levels. In *Proceedings of the 1st International Workshop on Pervasive Eye Tracking & Mobile Eye-Based Interaction* (Beijing, China) *(PETMEI '11)*. Association for Computing Machinery, New York, NY, USA, 37–42. https://doi.org/10.1145/2029956.2029967

[80] Qiushi Zhou, Brandon Victor Syiem, Beier Li, Jorge Goncalves, and Eduardo Velloso. 2024. Reflected Reality: Augmented Reality through the Mirror. *Proc. ACM Interact. Mob. Wearable Ubiquitous Technol.* 7, 4, Article 202 (2024), 28 pages. https://doi.org/10.1145/3631431

[81] Fengyuan Zhu, Ludwig Sidenmark, Mauricio Sousa, and Tovi Grossman. 2023. PinchLens: Applying Spatial Magnification and Adaptive Control-Display Gain for Precise Selection in Virtual Reality. In *2023 IEEE International Symposium on Mixed and Augmented Reality (ISMAR)*. 1221–1230. https://doi.org/10.1109/ISMAR59233.2023.00139